For College Applications: All highlighted sections were predominantly written by Srivishal (Abstract, Data, Analysis)

Team 3 - Kosmic Krakens
Orbit Determination Report

Determination of the Orbital Elements of Near-Earth Asteroid 1998 MX5 Using the Method of Gauss

By:
Kimberly Ferreira, Srivishal Sudharsan, and Velvet Wu

Summer Science Program
New Mexico State University

July 2023

I. ABSTRACT

This paper aims to redetermine the orbital path of the near-earth asteroid 1998 MX5 in order to update the accuracy of previously calculated orbital elements. By utilizing current observational data we aimed to test existing theoretical models from JPL's Horizons System[1]. Over the span of 5 weeks, we took numerous images of our asteroid and utilized various astronomical and mathematical techniques to redetermine the location of the asteroid. Using this data, the position of the earth in relation to the sun, and the times at which the images were taken, we utilized the Method of Gauss to determine 1998 MX5's 6 orbital elements: a, e, i, ω, Ω, and M(t_0). It was noted that our orbital elements had relatively low uncertainties, indicating high precision, and ranged from being 0.1% to 16.5% off from the theoretical model, depending on the orbital element. Thus, our results suggest that the asteroid may have either slightly changed paths since the orbital elements were previously calculated or errors may have been made when calculating our elements. Both perspectives will be explored in this paper.

II. INTRODUCTION

Some of the most defining events in Earth's history have ironically been the result of extraterrestrial objects. Approximately every hundred million years, an asteroid large enough to cause a mass extinction event collides with Earth. But smaller asteroids–100 tons of dust and sand-sized particles–hit Earth every day. And asteroids that aren't massive enough to cause an extinction event, but large enough to cause damage, hit Earth relatively often. Astronomers classify objects that come near Earth as near-Earth asteroids (NEAs), and asteroids that come close enough to hit Earth and are large enough to cause significant harm as potentially hazardous asteroids (PHAs). However, only an extremely small fraction of PHAs have been found–NASA estimates 20 to 30%. The purpose of our research is to determine the orbit of asteroid 1998 MX5 and determine its orbit–helping predict its future trajectory and its potential to collide with Earth. Our hypothesis was that the orbital elements predicted by JPL Horizons would fall within the range of uncertainty for the orbital elements calculated from our data and observations. We evaluated the success of our research on the difference between JPL's orbital elements and the orbital elements from our calculations.

The orbit of any object–stars, planets, asteroids–can be defined by six orbital elements: the semi-major axis a, eccentricity e, inclination I, longitude of ascending node Ω, longitude of perihelion ω, and mean anomaly M_0. Each orbit is an ellipse defined by semi-major axis and eccentricity. The inclination, longitude of ascending node, longitude of perihelion, and mean

[1] https://ssd.jpl.nasa.gov/horizons/app.html#/

anomaly define the elliptical plane of orbit in relation to a reference plane–in this case, the plane of orbit of the Earth around the Sun, called the ecliptic. Here, we state the equations used to calculate each element.

a. *Deriving orbital elements*

***Semi-major axis,* a**

The semi-major axis is calculated using the formulation

$$a = \left(\frac{2}{r} - \dot{r} \cdot \dot{r} \right)^{-1}$$

***Eccentricity,* e**

The eccentricity is calculated using the formulation

$$e = \sqrt{a - \frac{\left| r \times \dot{r} \right|^2}{a}}$$

***Inclination,* I**

The inclination is calculated using the formulation

$$I = arc\cos\left(\frac{(r \times \dot{r})_Z}{\left| r \times \dot{r} \right|} \right)$$

***Longitude of ascending node,* Ω**

The longitude of the ascending node is calculated using an expression of the angular momentum h, where $h = \sqrt{a(1 - e^2)}$. After some matrix multiplication, we find

$$\sin\Omega = \frac{h_X}{h \sin I}$$

$$\cos\Omega = -\frac{h_Y}{h \sin I}$$

Then, to eliminate quadrant ambiguity, we take inverse tangent of Ω, and our final expression for Ω is

$$\Omega = arc\tan\left(\frac{h_X}{-h_Y}\right)$$

Longitude of perihelion, ω

We first use expressions for the components of the Sun to asteroid vector r in Cartesian coordinates projected onto the auxiliary circle.

$$X = r\left[\cos(f+\omega)\cos\Omega - \cos I\sin(f+\omega)\sin\Omega\right]$$
$$Y = r\left[\cos I\cos\Omega\sin(f+\omega) + \cos(f+\omega)\sin\Omega\right]$$
$$Z = r\sin I\sin(f+\omega)$$

The magnitude of the vector r is $r = \sqrt{X^2 + Y^2 + Z^2}$.

We then manipulate the X and Z equations to find $f + \omega$. To find ω, we find f using the equation of orbit, and subtract from $f + \omega$.

i. Finding $f + \omega$

Manipulating the equation for Z, we get

$$\sin(f+\omega) = \frac{Z}{r\sin I}$$

Similarly solving the X equation, we obtain:

$$\cos(f+\omega) = sec\Omega\left(\frac{X}{r} + \cos I\sin(f+\omega)\sin\Omega\right)$$

We can now solve for $f + \omega$ without quadrant ambiguity using arctangent, as we did for Ω.

ii. Finding f

Now we use the orbital equation to find f.

$$r = \frac{a\left(1-e^2\right)}{1+e\cos f}$$

Solving for $\cos f$, we obtain:

$$\cos f = \frac{1}{e}\left(\frac{a\left(1-e^2\right)}{r} - 1\right)$$

To find $sinf$, we take the derivative of $cosf$ and substitute in for $\dot{f}$ using $h = r^2\dot{\theta} = r^2\dot{f}$. Eventually, we obtain:

$$\sin f = \frac{(r \cdot \dot{r})}{er}\sqrt{a(1-e^2)}$$

Again, we solve for f without quadrant ambiguity, then solve for ω as described above.

***Mean anomaly,* $\mathbf{M_0}$**

We first find E, the eccentric anomaly, at the time of the middle observation using the equations for the components of the Sun to asteroid vector *r*

$$x = acosE - ea$$

$$y = a\sqrt{1 - e^2}sinE$$

Note that this *x* and *y* differs from the *X* and *Y* used in calculating ω by the coordinate system being used. While *x* and *y* are the Cartesian coordinates of the asteroid, *X* and *Y* are the Cartesian coordinates for the asteroid projected onto the auxiliary circle centered on the ellipse.

Substituting into the equation $r^2 = x^2 + y^2$, we find $cosE = \frac{1}{e}(1 - \frac{r}{a})$. The quadrant ambiguity is eliminated by the fact that E is in the same half plane as *f*. The mean anomaly at the time of the middle observation is then $M_0 = E - esinE$.

b. Method of Gauss

In order to calculate the orbital elements, the position and velocity vectors are needed, as shown in section Ia. We have, from our observational data, the time of observation, right ascension, and declination for each of our three observations. Using the right ascension and declination, we can find the direction of $\vec{\rho}$, the unit vector pointing from Earth to the asteroid. Now, our issue is to find the magnitude of $\vec{\rho}$ so that we can use vector arithmetic to find the position vector $\vec{r}$, and subsequently the velocity vector $\dot{\vec{r}}$.

$$\vec{r_2} = \hat{\rho}\rho - \vec{R} \quad (1)$$

For this, we choose to use the Method of Gauss for determining orbital vectors, then use the orbital vectors produced from the method to generate the orbital elements as outlined in section Ia.

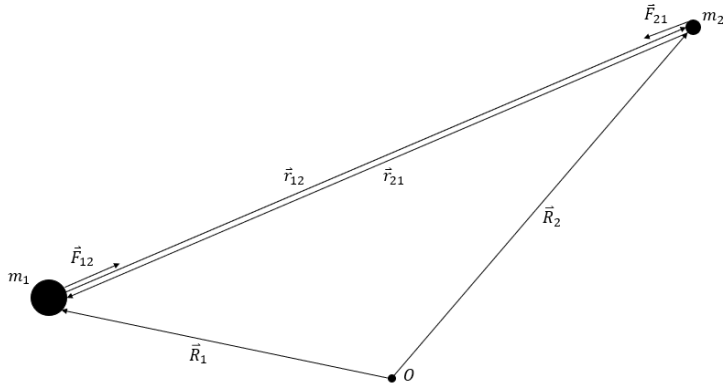

Diagram 1. Fundamental triangle representing earth, sun, asteroid vectors (Medium.com)

The Method of Gauss depends on an iterative process which updates orbital vectors $\vec{\rho}$, $\vec{r}$, and $\dot{\vec{r}}$ until the values converge to an acceptable value. The reason for iterations is the codependency of the $\vec{\rho}$, $\vec{r}$, and $\dot{\vec{r}}$. In order to calculate $\vec{r}$ and $\dot{\vec{r}}$, we need $\vec{\rho}$ (see equation 1). But, in order to calculate $\vec{\rho}$, we need $\vec{r}$ and $\dot{\vec{r}}$. As such, there is no way to directly calculate $\vec{r}$ and $\dot{\vec{r}}$ and we must iterate.

To start the iteration, we approximate $\vec{r}$ and $\dot{\vec{r}}$ using Kepler's 2nd law. Conservation of momentum dictates that all three position vectors for the asteroid–one from each observation–must be in the same plane. We can therefore express the position vector at the central observation $\vec{r}_2$ as some combination of the position vectors from the first and third observations, $\vec{r}_1$ and $\vec{r}_3$. So:

$$\vec{r}_2 = c_1\vec{r}_1 + c_3\vec{r}_3 \quad (2)$$

where c_1 and c_3 are constants.

For the same reason, all three velocity vectors are in the same plane as the position vectors, and we can express

$$\vec{r}_1 = f_1\vec{r}_2 + g_1\dot{\vec{r}}_2$$
$$\vec{r}_3 = f_3\vec{r}_2 + g_3\dot{\vec{r}}_2$$

where f_1, f_3, g_1, and g_3 are scalar time-dependent functions. After some manipulation, we obtain:

$$c_1 = \frac{g_3}{f_1 g_3 - g_1 f_3}$$
$$c_3 = \frac{-g_1}{f_1 g_3 - g_1 f_3} \quad (3)$$
$$\dot{\vec{r}_2} = d_1\vec{r_1} + d_3\vec{r_3}$$
$$\text{where } d_1 = \frac{-f_3}{f_1 g_3 - f_3 g_1}$$
$$\text{and } d_3 = \frac{f_1}{f_1 g_3 - f_3 g_1} \quad (4)$$

After some manipulation, we obtain

$$\rho_1 = \frac{c_1 D_{11} + c_2 D_{12} + c_3 D_{13}}{c_1 D_0} \quad \rho_2 = \frac{c_1 D_{21} + c_2 D_{22} + c_3 D_{23}}{c_2 D_0} \quad \rho_1 = \frac{c_1 D_{31} + c_2 D_{32} + c_3 D_{33}}{c_3 D_0} \quad (5)$$

We can then use Kepler's 2nd law to approximate initial values for c_1 and c_3 (see Appendix C), which can be used to solve for the initial ρ vectors using equation (5), which in turn can be used to solve for the initial magnitudes of the $\vec{r}$ vectors. We then again use Kepler's method to obtain an initial value for $\dot{\vec{r}}_2$.

Now, we start iterating. We first update our c values using equation (3). We then recalculate ρ values with our new c values, r values with our new ρ values (equation 1), and then perform the f and g series with the new $\vec{r}_2$ and old $\dot{\vec{r}}_2$ vectors. The f and g values are then plugged in to obtain the d_1 and d_3 values and in turn substituted in to recalculate $\dot{\vec{r}}_2$. This process is repeated until the difference between the current and previous ρ values is less than a specified threshold, at which point the $\vec{r}_2$ and $\dot{\vec{r}}_2$ vectors can be used to calculate orbital elements.

c. *Monte Carlo error estimation*

In order to obtain error estimations on our orbital elements calculated using Method of Gauss, a Monte Carlo error estimation is performed. This is done by randomly sampling normal distribution values for right ascensions and declinations from each observation, with root mean square uncertainties as the bounds for each distribution. Performing the Method of Gauss n times, each time with a new set of right ascensions and declinations sampled from the normal distribution, and storing the generated orbital elements, a normal distribution for each orbital element is obtained. The standard deviation of each normal distribution can then be calculated, producing the error estimation for each orbital element.

III. EQUIPMENT AND PROCEDURE

Observation of the 1998 MX5 was done using a 24'' Boller and Chivens telescope at Tortugas Mountain Observatory (TMO). This reflective telescope was operated from New Mexico State University's remote observing center over the course of 5 weeks. Observation shifts occurred every 4 days of observation. Prior to our observation shifts, we computed an ephemeris to predict our asteroid's location according to *NASA's Jet Propulsion Laboratory*'s online Horizons system. We recorded the right ascension, declination, APmag and elevation of the 1998 MX5 and used this data to detect focus stars and generate a finding chart.

During an observation shift, there are three general roles from observatory control, observing log and weather monitoring that are significant to a successful observing shift. Observatory control was responsible for running the computer to control the telescope and camera, assuring that the telescope was properly working and skewed to the region of the asteroid. This role was also in charge of making sure the data was being stored in the right directory. Observing log was responsible for keeping track of the data recorded from the telescope and entering the data to a digital observing log. Weather monitoring was in charge of monitoring the weather conditions and occasionally going outside to look at the sky. If it was immensely cloudy, it was important for the weather monitor to be on guard of the weather predictions and give notice to the observatory controller. All roles were equally important for a successful observing shift.

Many softwares programs such as *Focus Max*[2], *Maxlm DL*[3] and *ACP*[4] were operated in order to control the observatory. Firstly, we skewed the telescope to one of the focus stars and took a single exposure image using the Open (clear) filter. We used the same filter throughout all our observation shifts because the open filter takes in all wavelengths. Using *Maxlm DL*, we draw a square around a bright star and proceed to take continuous exposure images. The *Focus Max* panel aided in focusing the telescope by jogging in or out. Note that if the images have improved we will continue to increment in the direction selected until the focus worsens or vice versa. After the telescope is focused, we then slew the telescope to the asteroid according to the predetermined R.A and D.E.C coordinates and take a single exposure image to compare to our finding chart. Once it's confirmed, we set the camera to take a series of five 1-minute exposure 'Light' (science) images and one series for a "dark" filter. Taking a set of dark filter images (closing the camera shutter) is critical for data reduction since it subtracts the electrons that are thermally produced.

IV. DATA

During our project, we collected a total of 6 sets of images. However, after reducing each set of data, only 3 sets were clear enough to see our asteroid. As will be explained in section V. Data Analysis, the asteroid was identified by blinking through multiple images to see any moving body of light. Shown below are snapshots of our asteroid from each of the clear sets of data.

[2] https://www.focusmax.org/
[3] https://diffractionlimited.com/product/maxim-dl/
[4] http://acp.dc3.com/index2.html

a. Raw Asteroid Data

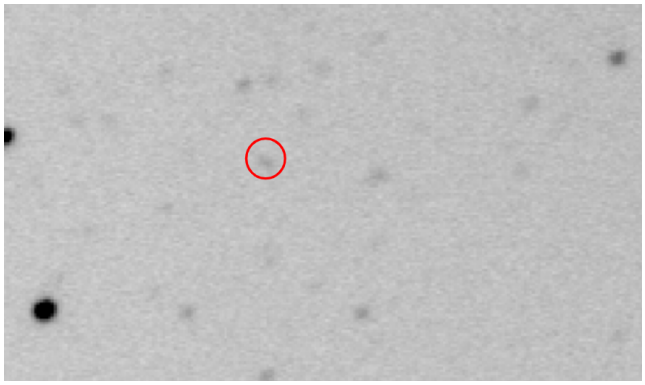

Image 1. Picture of asteroid on 2023-07-04 at 08:40:35.23

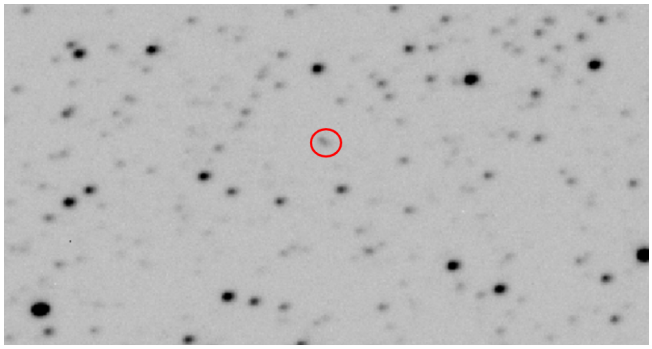

Image 2. Picture of asteroid on 2023-07-09 at 6:44:33.34

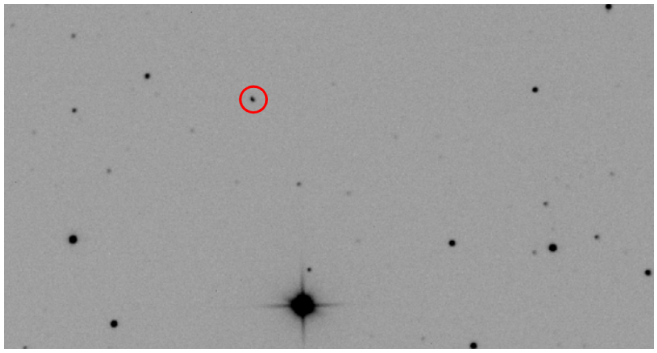

Image 3. Picture of asteroid on 2023-07-18 at 6:29:15.51

As shown in the images, the clarity of our asteroid greatly varied from Image 1 to Image 3. This was likely because our asteroid had a higher altitude towards the end of the month which allowed it to be seen more easily. To calculate the right ascension, declination, and apparent magnitude of our asteroid, we performed astrometry and photometry on each of our images as will be explained in section V. Data Analysis. The results are shown in the table below.

b. Astrometry and Photometry Data

Observation #	Date	Time (UTC)	RA (hh:mm:ss.ss)	Dec (dd:mm:ss.ss)	RA rms (seconds)	Dec rms (arcseconds)	Magnitude *	SNR
1	2023-07-04	8:00:15.94	18:39:40.06	-10:11:47.07	0.32	0.08	16.5	13.0
1	2023-07-04	08:40:35.23	18:39:40.95	-10:10:24.86	0.33	0.09	16.8	12.3
2	2023-07-09	07:22:57.08	18:43:34.46	-05:54:30.9	0.03	0.09	16.4	45.2
2	2023-07-09	6:44:33.34	18:43:33.479	-5:55:58.03	0.03	0.09	16.6	21.8
3	2023-07-18	7:10:29.10	18:52:58.632	+02:49:14.16	0.21	0.01	17.0	36.6
3	2023-07-18	6:29:15.51	18:52:56.866	+02:47:29.07	0.22	0.02	17.4	21.7

Table 1. Astrometry and Photometry data for 6 images (3 observations)
* Apparent Magnitude
# Observation used for Method of Gauss

The table above shows the date at which each image was taken, the midpoint time of the exposure, the right ascension (RA), declination (Dec), uncertainty of RA and Dec, apparent magnitude, and the signal to noise ratio of asteroid 1998 MX5. This data is extremely important in determining the orbit over time which was vital in calculating the final orbital elements which will be provided in the next section. For our Method of Gauss code only the highlighted observations were used as it only takes in 3 observations.

V. ANALYSIS

The following section utilizes figures from the data section and other sources to provide an in-depth breakdown of our data.

a. Data Reduction

After data collection, we used *Astro ImageJ* (AIJ)[5] , an image processing software in order to generate and assemble our raw images. The overall procedure for all science images was to reduce, align and run the images to identify our asteroid. Following the right procedure in AIJ,

[5] https://www.astro.louisville.edu/software/astroimagej/

such as creating master dark flats and flats, divides vignetting, dust donuts away, and subtracts the noise away. After data reduction, we begin the alignment process by selecting stars that have strong signals and do not overlap others. Finally, we can now run the images and closely analyze them. It's helpful to zoom in, pan, and invert the color or the x and y coordinates. If there is any movement through the stack of images, then we may have identified our asteroid. We then can record the RA and DEC coordinates from the reduced data.

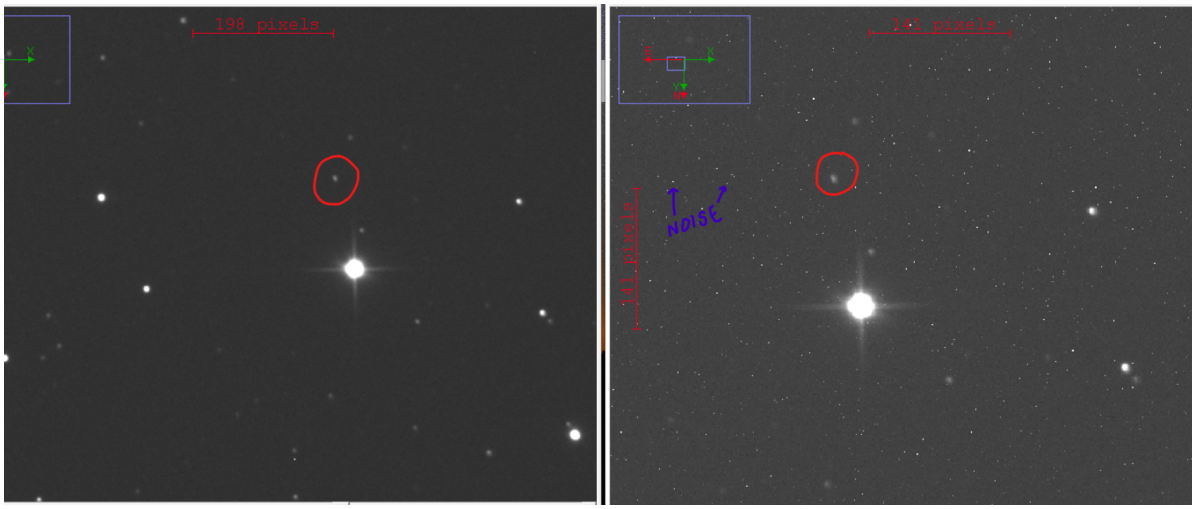

Image 4 and 5. Picture of Asteroid (reduced on left and raw on right): 2023-07-18 7:06:00

b. Astrometry

Table 1 presents the right ascension and declination of our asteroid at 6 different times. To obtain these values we inputted the images into Astrometry.net after reducing. Astrometry.net matches up star patterns seen in the image with a database of known stars and their right ascensions and declinations. Utilizing this, they then map out every (X,Y) coordinate on the image to a (RA, Dec). This new image is outputted and we used a software called AstroimageJ. After that we had to blink through our previously reduced images to find the asteroids (X,Y) on the image we were analyzing. This then gave us the (RA, Dec) of the asteroid at every time in the table. We purposely chose times on the same day that were relatively far apart to allow the asteroid to move a significant distance which would give relatively different (RA, Decs) and allow us to see the path over a longer time period. Not only are these values required to calculate the orbital elements, but they also were reported to the Minor Planet Center in order to improve their predicted orbit of asteroid 1998 MX5. Additionally, as a part of astrometry, we calculated the uncertainty of our RA and Dec values.

c. Photometry

In order to determine the apparent visual magnitude of our asteroid, we first perform centroiding to determine the visual center of mass of any sky object. On any point source in an image, an aperture containing all pixels in the source is set, with an annulus containing background sky pixels around it. Averaging the pixel values in the annulus and subtracting the average from each pixel in the aperture to remove background noise, we obtain the signal of the point source. Then, a weighted mean is used to calculate the coordinates of the center of the point source. Using the gain, read noise, sky background noise, and signal, the signal-to-noise ratio can also be calculated.

To find the visual magnitude of the asteroid in each observation, stars in images from each observation are located and their approximate coordinates in the image are recorded. Their visual magnitudes are also recorded through analysis in *SAOImageDS9*[6]. Centroiding is performed on the recorded stars to find each star's signal, and a linear regression of apparent visual magnitude recorded from *SAOImageDS9* versus the logarithm of the signal is performed. The asteroid's signal is also calculated, and the linear regression is used to predict the asteroid's apparent magnitude.

d. Method of Gauss, Monte Carlo, and Sources of Error

As described in Section II. Introduction, the Method of Gauss takes in the position vector of the earth in relation to the Sun as well as the time at which the data was taken. The position vector of the earth in relation to the Sun at each of our observation images was taken from JPL Horizons. Additionally, the RA and Dec of the asteroid at the time of observation were found via the astrometry explained in section Vb. We then used the Kepler method (Appendix C) to find our initial position and velocity vector. After that, to find our f and g values we utilized the 4th-order Taylor series (Section II. Introduction) which allowed us to iterate through the Method of Gauss and determine our final orbital elements. Note that each person wrote their own code which resulted in varying orbital element results. The final results are shown below along with their uncertainties, JPL horizons predictions, and how far off our values were from the model.

Orbital Element Data

Orbital Elements for Asteroid	Srivishal S.		Kimberly F.		Velvet W.		JPL Prediction	% off from JPL values *	Relative Uncertainty**
	value	uncertainty	value	uncertainty	value	uncertainty			
a (au)	3.3	0.2	3.9	0.3	3.3	0.2	2.9	16.5%	0.06

[6] https://sites.google.com/cfa.harvard.edu/saoimageds9

e	0.64	0.02	0.69	0.02	0.64	0.02	0.61	7.0%	0.03
i°	10.0	0.3	10.699	0.003	10.0	0.2	9.7	5.1%	0.03
ω°	56.9	0.2	56.761	0.002	56.9	0.1	55.9	1.6%	0.004
Ω °	265.42	0.09	265.61	0.10	265.42	0.08	266.5	0.4%	0.0003
$M(t_0)$ °	355.9	0.4	355.1	0.5	355.9	0.5	355.1	0.1%	0.001
# of Monte Carlo Runs	1,000,000		10,000		1,000,000				

Table 2. Orbital element data and uncertainties for each team member
* Calculated by taking the absolute value of the JPL orbital element divided by the average of all 3 group members' orbital elements and multiplying by 100
** Calculated by using 1st column of data and dividing uncertainty by the value
Green highlight indicates that for at least 1 students data, the JPL value lied in the range of the uncertainty for that orbital element

The table above shows all 6 orbital elements and the values that each of our group members calculated for the element. Importantly, we can see that our values were all relatively precise as shown by the low uncertainty values. However, as shown by the last column our values were slightly off from the JPL predicted values. If we look at each student's data and take the most accurate one for each orbital element (closest to the theoretical model) then we see that for

. There are a couple of reasons for this. First off, there may have been a systematic code error as the 2nd set of orbital elements vary from the other ones. We believe that since this 2nd set of values is farther off from the predicted values than the other two, it may have suffered a code error which skewed the results. Another error may have been from our data collection as our asteroid was quite faint (~17) throughout the weeks. Other errors may have come from the astrometry which could have resulted in slightly inaccurate right ascensions and declinations

which could have affected our final results. Another possibility is that the asteroid may have changed paths since the elements were last calculated. This may have occurred due to a large impact that changed its course. However, this is quite unlikely as Team 9 at SSP had calculated values that were extremely close to JPL's model for the same asteroid. Additionally, impacts that change the orbit to this magnitude are extremely rare due to the vastness of space. To find the family of near-earth asteroids that our asteroids belong to we have to look at our a (semi-major axis) and q value (a(1-e)). According to our data, the value ranges from 3.3-3.9 (likely on the lower side due to the reasons explained above). Using our e and a value we calculated the q value to be 1.18. Since this is below 1.272 we can conclude that our asteroid is an Amor.

Monte Carlo

The uncertainty values in Table 2 were found via the Monte Carlo method described in Section IIb. After performing the Monte Carlo method with 1,000,000 iterations, we created histograms (Appendix C) which visualize the spread of the data. As expected, it follows a normal distribution which helps confirm the accuracy of our uncertainties. The table below provides the mean value for each orbital element from Graphs 1-6.

Orbital Element	Mean Value
Semi Major Axis (AU)	3.29
Eccentricity	0.64
Inclination (°)	10.04
Longitude of Perihelion (°)	56.93
Longitude of Ascending Node (°)	-94.58
Mean Anomaly (°)	353.57

Table 3. Mean values of orbital elements from Monte Carlo run of 1,000,000 iterations

As compared to our final orbital elements from Table 2, we see that these values match up. This also confirms that our uncertainties are accurate.

VI. CONCLUSION

Originally we hypothesized that the JPL values would lie in the range of our uncertainties. If we look at all 3 students' data we can see that when looking at the most accurate data point for each orbital element only 2 of JPL's predicted values lie in the uncertainty of our values, as shown by the green highlight in Table 2. From the data, we see that our orbital elements differ from JPLs

ranging from 0.1% to 16.5%. As further explained in the previous section this may have been caused by error in code, observational errors, miscalculations, or changes in the asteroid's orbit. All of these would have affected our quantitative results as they would not only cause inaccurate orbital elements but may have also affected our uncertainties. Our uncertainties did seem to be quite low ranging from 0.02-0.4. Indeed as shown in Table 2 our relative uncertainties were extremely low ranging from 0.0003-0.06. Determining accurate orbital elements is important to ensure that the asteroid does not hit Earth in the near future.Although it is unlikely for asteroids to hit Earth, it is important to study near-Earth asteroids to prevent potential risks or catastrophic events. The purpose of our research was to conduct a study of a near-Earth asteroid 1998 MX5, to determine its orbit and its future trajectory. Although we did determine the future orbit there is more research to help understand its risk and apply it to more asteroids. In the future, we could expand this research by determining if there is a risk that asteroid 1998 MX5 will hit the Earth. This would help us prepare for the event by creating technology to potentially deflect the asteroid's path. Additionally, we could expand this research by observing other near-earth asteroids. Although less urgent, it could also be expanded to main belt asteroids which would give us more knowledge of the outskirts of our solar system. Researching these seemingly faraway objects will expand our understanding of our universe while providing early warnings of potentially disastrous collisions.

ACKNOWLEDGEMENTS

Team 3 would like to express their deepest gratitude and appreciation to all who aided us to have successful research experience. Our sincerest thanks to Dr. Rengstorf, Dr. Andersen and Dr. Bauer for giving us the proper tools and skills to conduct research. Their lectures were a great help and reference that was used throughout the entire lecture. Huge thanks to Lara, Kathyrn, Joel and Benj, who always encouraged us to try our best, answered many questions and assisted us in the many mistakes we made over the course of the program. Special thanks to Jon Holtzman for giving us, the Summer Science Program, the opportunity to access the Tortugas Mountain Observatory to conduct research. Our research project would not have been possible without those who supported the participants of the Summer Science Program.

REFERENCES

Nasa Jet Propulsion Laboratory, “Horizons System” (2023)
Horizons System (nasa.gov)

American Museum of Natural History, “Mass Extinction: What Happened 65 Million Years

Ago?”https://www.amnh.org/exhibitions/dinosaurs-ancient-fossils/extinction/mass-extinction

NASA Content Administrator (March 31, 2014), “Asteroid Fast Facts” https://www.nasa.gov/mission_pages/asteroids/overview/fastfacts.html (Aug 7, 2017)

Medium - How to Solve the Two-Body Problem (Feb 15, 2022), “Learn the fundamentals of orbital mechanics by deriving the equations of motion for a two-body system

https://medium.com/illumination/astrodynamics-two-body-problem-ec2c5e148184

APPENDICES
Appendix A

MPC REPORT

COD XXX
CON A. W. Rengstorf
CON [adamwr@pnw.edu]
OBS K. Ferreira, S. Sudharsan, V. Wu
TEL Size: 0.6m f/5.6 reflector + CCD
NUM 3
ACK Team 3 - 1998 MX5

65996	C2023 07 04.33352	18 39 40.06	-10 11 47.1	16.5 R	XXX
65996	C2023 07 04.36152	18 39 40.95	-10 10 24.9	16.8 R	XXX
65996	C2023 07 09.30761	18 43 34.46	-05 54 30.9	16.4 R	XXX
65996	C2023 07 09.28094	18 43 33.48	-05 55 58.0	16.6 R	XXX
65996	C2023 07 18.29895	18 52 58.63	+02 49 14.2	17.0 R	XXX
65996	C2023 07 18.27032	18 52 56.87	+02 47 29.1	17.4 R	XXX

Appendix B

Graph 1. Normal distribution of semi major axis values using Monte Carlo method of error estimation

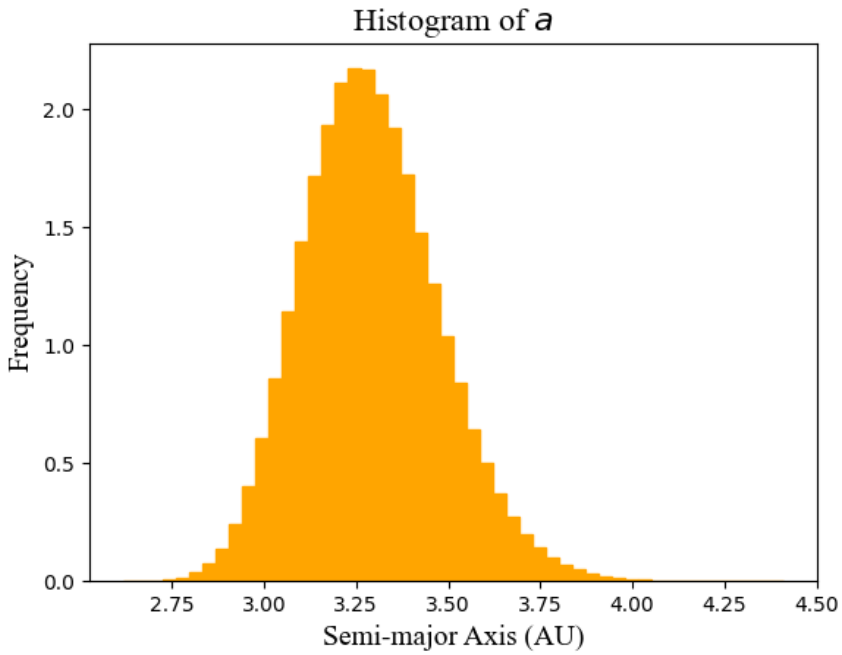

Graph 2. Normal distribution of eccentricity values using Monte Carlo method

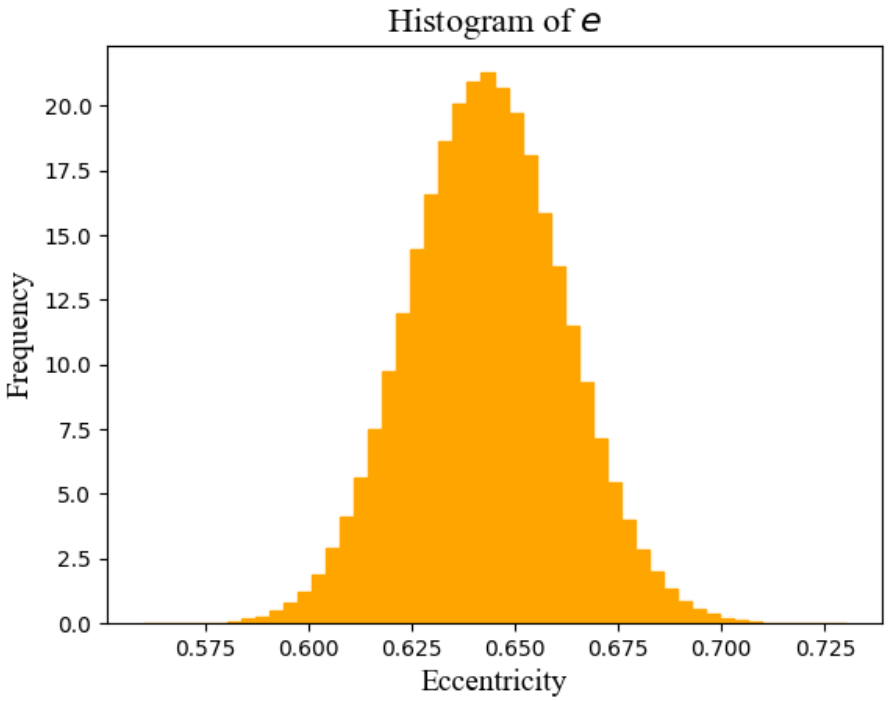

Graph 3. Normal distribution of inclination values (in degrees) using Monte Carlo method

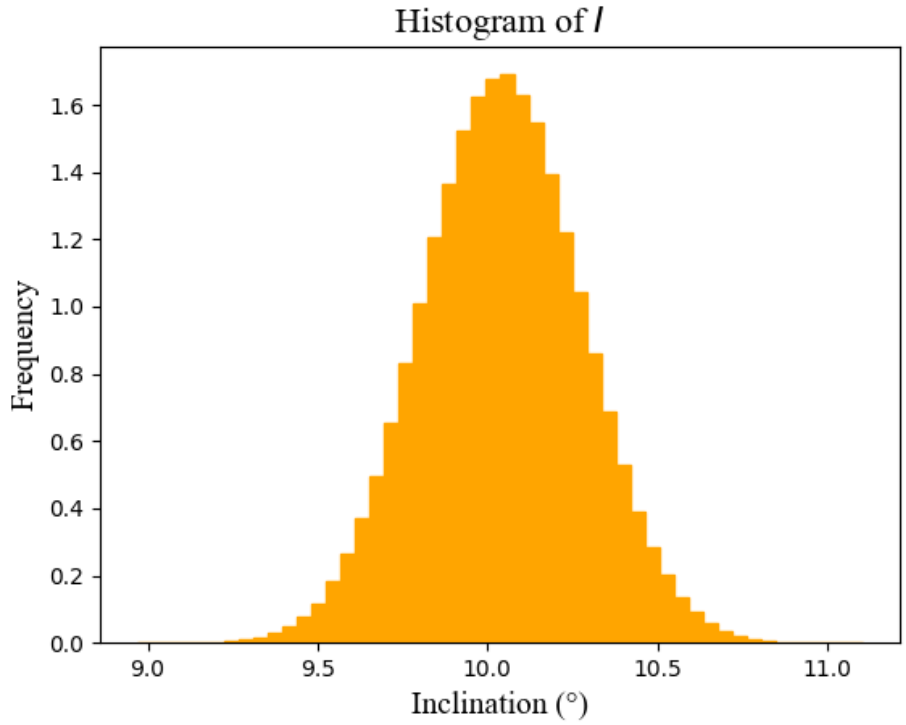

Graph 4. Normal distribution of longitude of perihelion values (in degrees) using Monte Carlo method

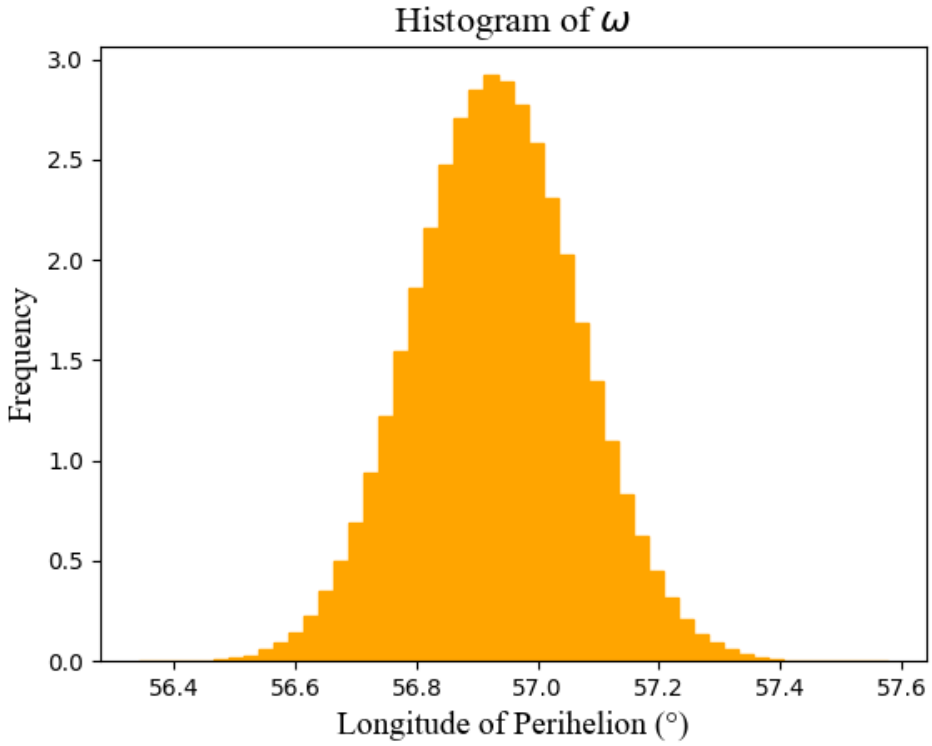

Graph 5. Normal distribution of longitude of ascending node (in degrees) Monte Carlo method

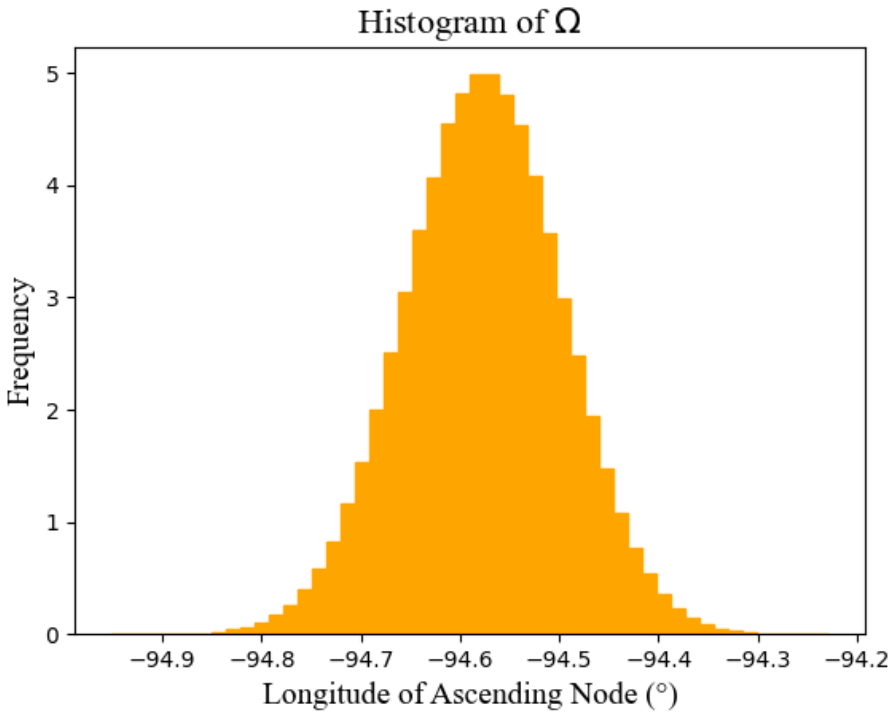

Graph 6. Normal distribution of longitude of mean anomaly values (in degrees) using Monte Carlo method

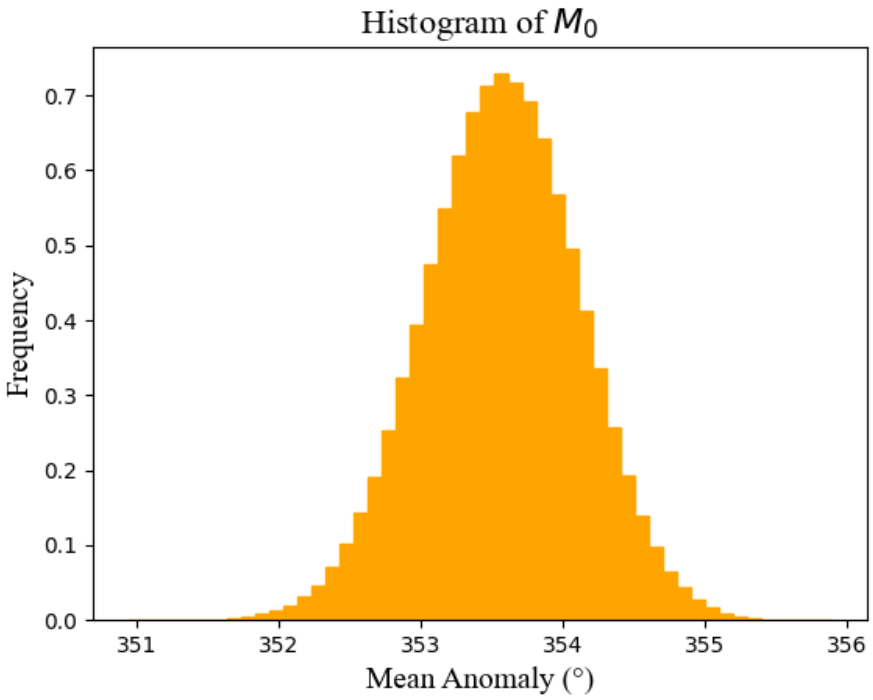

Appendix C: Using Kepler's 2nd Law to Approximate $\mathbf{r}_2$ and $\dot{\mathbf{r}}_2$

For any three observations at times t_1, t_2, and t_3, the areas B_1 and B_3 swept out in time intervals $t_2 - t_1$ and $t_3 - t_2$ are equal and sum to area B swept out in time $t_3 - t_1$. So:

$$\frac{B_1}{t_2 - t_1} = \frac{B_3}{t_3 - t_2} = \frac{B}{t_3 - t_1}$$

We then assume triangular areas are a close enough approximations of the areas B, B_1, and B_3, and use the vector cross product of Sun to asteroid vectors to calculate area. So:

$$A = \frac{1}{2}|\vec{r_1} \times \vec{r_3}|$$
$$A_1 = \frac{1}{2}|\vec{r_1} \times \vec{r_2}|$$
$$A_3 = \frac{1}{2}|\vec{r_2} \times \vec{r_3}|$$

After some manipulation, we obtain:

$$c_1 = \frac{t_3 - t_2}{t_3 - t_1}$$
$$c_3 = \frac{t_2 - t_1}{t_3 - t_1}$$

We then use c_1 and c_3 to find ρ using equation (5) and then use equation (1) to calculate $\vec{r}_2$, $\vec{r}_1$, *and* $\vec{r}_3$. We then use these vectors to approximate $\dot{\vec{r}}_2$.

$$\dot{\vec{r}}_2 = \frac{\vec{r}_3 - \vec{r}_1}{\tau}$$

Appendix D
f and *g* functions

In order to approximate $\vec{r}$, we begin with a Taylor series expansion about the position vector at the central observation time, $\vec{r}_2$.

$$\vec{r}_i = \vec{r}_2 + \dot{\vec{r}}_2 \tau_i + \frac{1}{2} \ddot{\vec{r}}_2 \tau_i^2 + \ldots$$

After some manipulation, grouping, and expansion, we find:

$$f_i = 1 - \frac{1}{2} u \tau_i^2 + \frac{1}{2} uz \tau_i^3 + \frac{1}{24} \left(3uq - 15uz^2 + u^2 \right) \tau_i^4 + \ldots$$

$$g_i = \tau_i - \frac{1}{6} u \tau_i^3 + \frac{1}{4} uz \tau_i^4 + \ldots$$

where tau represents the gaussian time of the observation.

$$u = \frac{\mu}{r_2^3}, \; z = \frac{\vec{r}_2 \cdot \dot{\vec{r}}_2}{r_2^2}, \; q = \frac{\vec{r}_2 \cdot \dot{\vec{r}}_2}{r_2^2}$$